BioSystems 124 (2014) 75–85

Contents lists available at ScienceDirect

BioSystems

journal homepage: www.elsevier.com/locate/biosystems

Comparison of the molecular topologies of stress-activated transcription factors HSF1, AP-1, NRF2, and NF-κB in their induction kinetics of HMOX1

Tessa E. Pronk [a,b,*], Jochem W. van der Veen [a,b], Rob J. Vandebriel [a], Henk van Loveren [a,b], Erik P. de Vink [c], Jeroen L.A. Pennings [a]

[a] Centre for Health Protection, National Institute for Public Health and the Environment (RIVM), P.O. Box 1, NL-3720BA Bilthoven, The Netherlands
[b] Department of Toxicogenomics, Maastricht University, Maastricht, The Netherlands
[c] Department of Mathematics and Computer Science, Eindhoven University of Technology, Eindhoven, The Netherlands

ARTICLE INFO

Article history:
Received 20 April 2014
Received in revised form 30 August 2014
Accepted 4 September 2014
Available online 6 September 2014

Keywords:
Modelling
Gene regulatory network
Oxidative stress
Denatured protein
HMOX1
Network topology
Transcription factor

ABSTRACT

For cells, reacting aptly to changes in their environment is of critical importance. The protein Heme oxygenase-1 (HMOX1) plays a critical role as a guard of cellular homeostasis and is considered as a reliable indicator of cellular oxidative stress. A better insight in the regulation of HMOX1 would assist in understanding the physiological role of HMOX1 as well as improving functional interpretation of the gene as a biomarker in toxicogenomics. Remarkably, as many as four transcription factors are known to regulate the HMOX1 gene: HSF1, AP-1, NRF2, and NF-κB. To investigate induction kinetics of these transcription factors, we constructed mathematical simulation models for each of them. We included the topology of the known interactions of molecules involved in the activation of the transcription factors, and the feedback loops resulting in their down-regulation. We evaluate how the molecular circuitries associated with the different transcription factors differ in their kinetics regarding HMOX1 induction, under different scenarios of acute and less acute stress. We also evaluate the combined effect of the four transcription factors on HMOX1 expression and the resulting alleviation of stress. Overall, the results support the assumption of different biological roles for the four transcription factors, with AP-1 being a fast acting general stress response protein at the expense of efficiency, and NRF2 being important for cellular homeostasis in maintaining low levels of oxidative stress.

1. Introduction

Oxidative stress is believed to underlie the etiology of numerous human conditions. Under a wide range of stressful conditions, the protein Heme oxygenase-1 (HMOX1) plays a critical role in the maintenance of cellular homeostasis. HMOX1 is able to alleviate stress caused by reactive oxygen species (ROS) as its products have potent antioxidant and anti-inflammatory properties as well as signalling capabilities. As many diseases are accompanied by conditions of oxidative stress, and HMOX1 is one of the most sensitive and reliable indicators for several pathological conditions related to cellular oxidative stress, the modulation of HMOX1 activity is of potential therapeutic value (Ryter et al., 2006). In toxicogenomics, the up-regulation of *Hmox1* is an important indicator for the skin sensitizing potential of a chemical (Natsch, 2009; van der Veen et al., 2013; Vandebriel et al., 2010). Possibly, the beneficial effects of HMOX1 in some systems may be limited to narrow windows of concentrations (Suttner and Dennery, 1999 Walther et al., 2012), increasing the need for a thorough understanding of its induction. A better insight in the regulation of HMOX1 may assist in understanding the biological role of HMOX1, as well as improving the functional interpretation of this gene as a biomarker. The variability in response could be caused by the multitude of stress-activated recognition sites contained within the *Hmox1* promoter. No less than four known transcription factors are able to directly induce the expression of *Hmox1* (Alam and Cook, 2007): HSF1, AP-1, NRF2, and NF-κB, which we will discuss in the following paragraphs.

HSF1 is a regulator of heat shock proteins (HSPs). The heat shock response is a molecular response to non-native and damaged or misfolded proteins (Szymanska and Zylicz, 2009). HSPs act either as chaperones to assist in proper folding, or as an escort for the

* Corresponding author at: Centre for Health Protection, National Institute for Public Health and the Environment (RIVM), P.O. Box 1, NL-3720BA, Bilthoven, The Netherlands.
E-mail address: tessa.pronk@gmail.com (T.E. Pronk).

http://dx.doi.org/10.1016/j.biosystems.2014.09.005
0303-2647/

proteins to the proteasome for degradation. Under normal conditions, HSF1 exists as an inactive monomer in a complex with the HSP Hsp70. Upon the formation of denatured proteins (DP), HSP70 is released from the complex to carry out its chaperone function with the DP. The now released HSF1 trimerizes and is transported into the nucleus where it is hyperphosphorylated. This enables HSF1 to bind to heat shock elements in the DNA, initiating the expression of HSPs. Its decline as an active transcription factor is initiated through a negative feedback loop with its gene product HSP70, which binds to the HSF1 transactivation domain. Although humans do not appear to have a consensus binding element for HSF1 in the promoter site for HMOX1 (Alam and Cook, 2007), there is evidence that a distal promoter site takes over this task under some conditions (Alam and Cook, 2007). To support this claim, a common expression pattern of heat shock induced proteins and HMOX1 in chemical induction of sensitization has been suggested (Pronk et al., 2013).

AP-1 is a transcription factor composed of proteins belonging to *c*-FOS, *c*-JUN and/or ATF family. It regulates gene expression in response to a variety of stimuli. Its regulation occurs in two ways: firstly by phosphorylative activation of the constituents of AP-1 that are already present, secondly by rapid and transient transcription (and translation) of the constituents based on cellular stimuli transferred by signalling pathways (Miller et al., 2010; Karin, 1995).

The NRF2 antioxidant response pathway is the primary cellular defence mechanism against the cytotoxic effects of oxidative stress. NRF2 increases the expression of several detoxifying and antioxidant enzymes. Under normal conditions, NRF2 is sequestered in the cytoplasm by KEAP1 leading to fast degradation. In the nucleus, the binding of NRF2 to the antioxidant response element (ARE) is inhibited by BACH1. Under oxidative stress conditions, ROS binds to KEAP1 and BACH1, releasing NRF2 to travel to the nucleus where it initiates transcription of anti-oxidative genes by binding to ARE (Reichard et al., 2007). When ROS is cleaned up, the system automatically returns to steady state as BACH1 and KEAP1 are no longer bound by ROS and resume the inhibition of NRF2 binding.

NF-κB is a group of related transcription factors found in almost all vertebrate animal cell types. It is involved in cellular responses to various stimuli. Under normal conditions, IκBA sequesters the NF-κB in an inactive state in the cytoplasm by masking nuclear localization signals. Its activation is initiated by the induction of activated IKK-dependent degradation of IκBA proteins. Activated NF-κB translocates to the nucleus, where it induces the expression of its own repressor IκBA, re-inhibiting NF-κB (for a detailed description, see Ruland, 2011).

Over the past decades, a reasonable understanding of the workings of the molecular circuitry of these four transcription factors in the induction by oxidative stress has been achieved. The details of their functioning in terms of kinetics and thresholds is hard to predict by their topology but can effectively be determined by modelling.

Models describing the activity of the individual transcription factors have been proposed. The response to unfolded protein by HSF1 has been modelled on several occasions (Szymanska and Zylicz, 2009; Petre et al., 2009; Peper et al., 1998; Rieger et al., 2005). The same applies to the NF-κB response (Ihekwaba et al., 2004; Lipniacki et al., 2004; Hoffmann et al., 2002). The AP-1 response was modelled by Miller et al. (2010). Although the model of NRF2 is well described in literature, we were not able to find an explicit mathematical model. Despite the usefulness of these models as they are, their difference in detail and difference in values of (fitted) parameters makes it difficult to compare them directly with regard to the induction kinetics of HMOX1. We therefore use the HSF1 model of Szymanska and Zylicz (2009) as a template, to model the molecular circuitries of the other transcription factors. This template is essentially as follows: a stressor (ROS or ROS-derived DP) leads to activation (by homo- or heteromeric complex formation or dissociation) of signalling protein or complex, which leads to transcriptional regulation of Hmox1 and (for some of the models) a signalling protein as well. This leads to reduced levels of the stressor, thus closing the circuitry. The resulting models have a low level of complexity, while they still capture the basic characteristics of the system. The novelty of this approach lies in the fact that the level of abstraction for each model now is comparable, as are the transcription-, translation- and biochemical reaction rates and protein abundances. This allows us to compare the transcription factors exclusively on the topology of the interacting molecules in their circuitry. This comparison also enables us to assess the value of the different transcription factors when combined in their effect on HMOX1 induction and ROS and DP removal under various stress situations, shedding light on their individual physiological role.

2. Material and methods

2.1. Parameters and molecular circuits

We take the model of Szymanska and Zylicz (2009) on the denatured protein response by the HSF1 molecular circuit as a template for our models. We adjust the model only slightly by introducing HMOX1 into the model, as a HSF-inducible molecule, in addition to HSP70. Moreover, parameter l4 (transcript degradation rate) is introduced. In the original model, this was integrated in parameter k4 (translation rate). The separation between transcript degradation rate and translation rate enables us to model mRNA transcript levels separately from the corresponding protein levels and change transcription and translation rates independently in future models, if required. Listed in Table 1 are parameters as used in the model of Szymanska and Zylicz (2009) with our adaptations.

In the model of Szymanska and Zylicz (2009), association and dissociation rates are set to mimic the known preferred state, i.e. if two proteins are known to mostly occur as a complex, the association rate in the model should exceed the dissociation rate. To make all models comparable in terms of initial values and rates, we transfer the parameters used in the HSF1 model of Szymanska and Zylicz (2009) to the other models, thereby introducing the same level of abstraction to the AP-1, NRF2, and NF-κB models. Now only the topology of the biochemical reactions is different for each transcription factor model. In Fig. 1, we show the biochemical reactions between molecules for each molecular circuit. In Table 4 the complete models with all biochemical reactions and their parameters can be found. In concordance with the model of Szymanska and Zylicz (2009), the model does not explicity model cellular compartments nor phosphorylation steps. To obtain the models in Fig. 1, Table 2 the models as described in Section 1, as generally agreed upon, are taken as a guideline.

2.2. Reactive oxygen species (ROS) and denatured protein (DP) exposure

We simulate a single surge of oxidative stress by introducing exposure to ROS and DP, such as would be the case after exposure to a toxicant, especially one with skin sensitizing potential (Vandebriel et al., 2010; van der Veen et al., 2013; Saito et al., 2013). We model ROS and DP to increase relatively fast and then slow down after a certain exposure time (Miller et al., 2010). We use the following formula (Caton et al., 1999) to simulate the total stress exposure *EXP* at each time *t*:

Table 1
Parameters used in the model. Rate parameters and initial values are based on the model of Szymanska and Zylicz (2009). Exposure parameters are fitted, loosely based on Miller et al. (2010).

Parameter	Value	Description
k1	0.42	Binding of two molecules
l1	0.005	Dissociation of two molecules
k3	0.023	Association of trimers
l3	0.00575	Dissociation of trimers
k4	0.035	Translation rate
l4	0.035	Degradation rate of mRNAs
k6	0.023	Dimer synthesis from existing dimer plus release, preferred state
l6	0.00036	Dimer synthesis from existing dimer plus release, non-preferred state
k10	0.014	DP or ROS cleanup rate at binding respectively to HSP70 and HMOX1
l10	0.013	Degradation rate of proteins
k7	0.035	Binding transcription factor to binding site
l7	0.035	Dissociation of transcription factor and binding site
k8	0.035	Transcription rate
k11	0.002	DP production from ROS
l11	0.1	Parameter of signal increase from ROS increase
P_0	20	Shape parameter stress exposure
P_1	1	Shape parameter stress exposure
P_2	3	Shape parameter stress exposure
EXP_{time}	360 min	Total length of stress exposure
EXP_{tot}	30	Total stress exposure
ROS_{part}	0.7	Part of stress exposure that is reactive oxygen species
DP_{part}	0.3	Part of stress exposure that is denatured protein
Timestep	0.1 min	Minimum time step
Molecules	1	Initial value of proteins

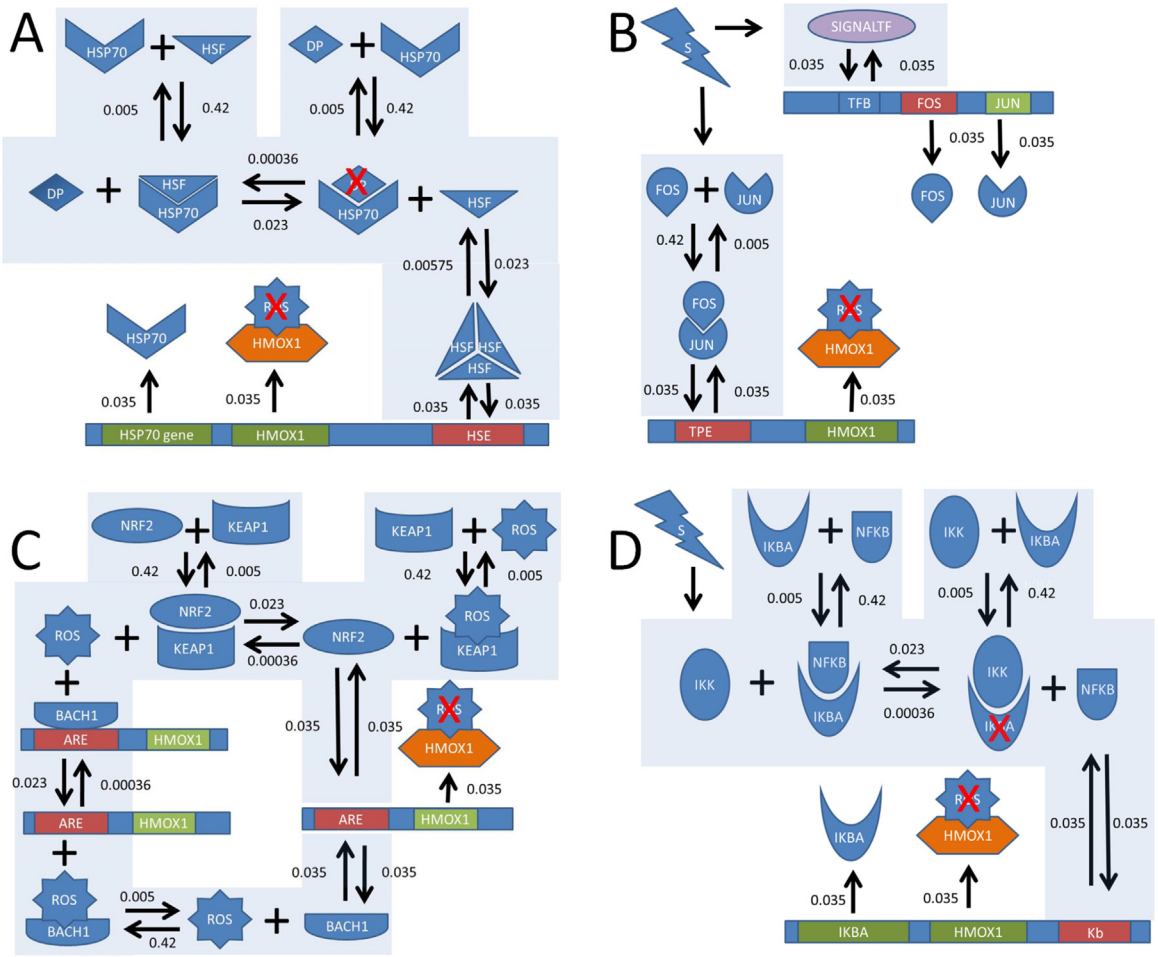

Fig. 1. Modeled topologies and biochemical reaction rates (arrows) for the molecular circuits capable of inducing HMOX1: (A) The HSF1 molecular circuit. (B) The AP-1 molecular circuit. (C) The NRF2 molecular circuit. (D) The NF-κB molecular circuit. Bars represent mRNA, other shapes represent proteins or other molecules. For a description of names, see Table 2.

$$\mathrm{EXP}_t = p_0 \times \frac{\mathrm{EXP_{tot}}}{\mathrm{EXP_{time}}} \times \left(\frac{t}{\mathrm{EXP_{time}}}\right)^{p_1} \times \left(1 - \frac{t}{\mathrm{EXP_{time}}}\right)^{p_2} \quad (1)$$

Here $\mathrm{EXP_{tot}}$ is the total stress exposure (consisting of ROS and DP), $\mathrm{EXP_{time}}$ is the total length of that exposure, and p_0, p_1, p_2 are shape parameters. Here, the shape parameter p_0 is given in terms of p_1 and p_2 by the integral:

$$p_0 = \left(\int_0^1 dx \times x^{p_1}(1-x)^{p_2}\right)^{-1} \quad \text{with} \quad x = \frac{t}{\mathrm{EXP_{time}}} \quad (2)$$

This formula allows us to model the duration of exposure to stress $\mathrm{EXP_{time}}$ and total exposure $\mathrm{EXP_{tot}}$ independently, as well as change the shape of the ROS induction over time with the parameters p_1 and p_2.

As many inducers of ROS also induce denaturation of proteins, we assume the stress to consist of both DP and ROS toxicity. Moreover, as ROS itself is also a cause for denaturation of proteins, we assume the DP to also increase with a fraction of total ROS at any time t. Thus, toxicant exposure can lead to denatured proteins by direct as well as indirect mechanisms, each with a separate kinetic parameter. The signal S (see 'S' in the lightning symbol in Fig. 1) activates IKK, FOS and JUN by phosphorylation. The strength of S is assumed to follow the ROS induction at each time t.

2.3. Model run

We run the models with a variable time step to prevent overestimation of the changes in state while keeping the time for simulation as short as possible. If the relative rate (calculated as rate/state) of a molecule exceeds 0.01, the time step is adjusted to half its size. This is repeated up to a maximum of three times. After careful evaluation, this approach proved to be sufficient for all of the considered models and rates in the sensitivity analysis. The simulation of ROS and DP exposure only starts after the steady-state of each individual model has been reached.

For model evaluation, we first evaluate the steady-state behaviour of the four models and compare them to reported steady-state behaviour from the literature, where possible. In addition, we assess the sensitivity of each of the four models to a 25% change in parameter values. Thirdly, we test the models with regard to their kinetics under different stress scenarios, namely more or less severe stress, and a shorter or longer period of stress. After considering these models individually, we assess the kinetics of the four different transcription factor circuits when combined in a single model at default parameter values. For this combined model, we test the influence of three toxicant exposure scenarios on the system, namely the shape of the exposure curve (see Eq. (1)); a change to relatively more stress by DP than by ROS; and an increase in both ROS and DP stress.

3. Results

3.1. Steady-state values

As a first step to study the robustness of the model, we determined how a model would approach a steady-state situation of a system under natural conditions. For NF-κB, literature states that 85% of IκBα is bound to NF-κB and 15% is free under normal conditions (Rice and Ernst, 1993). The model shows a similar result, as at steady state 84.4% IκBα is bound to NF-κB, while 15.6% is free. For HSP70, qualitative results are reported in literature stating that most HSP70 (HSP90) is bound to HSF1 at steady-state (Szymanska and Zylicz, 2009). This fits with our model in which also most (88%) HSP70 is bound to HSF1 at steady-state. For NRF2, we did not find information on steady-state conformations. However, we would expect the NRF2 transcription factor to be largely inactive. In our model, at steady state NRF2 was indeed found to be mostly in the inactive conformation of NRF2_KEAP1 (89.2%), with 9.8% free NRF2 and only a small part in the active conformation of NRF2_ARE (1%). Moreover, BACH1 is mostly bound to ARE (89.2%) with 10.7% free BACH1. This shows that in our model at steady-state NRF2 is mostly inactive, as one would expect, and moreover the transcription initiation site ARE is for the larger part not available for binding by NRF2. For AP-1, the model as constructed does not allow for comparisons at the steady-state level. We assume that in the simulation, the activated molecules start at zero and only increase after a stress-induced signal (similar to IκK in the NF-κB model). So in this model there is no feedback loop to balance conformations and this system has to return to steady-state (zero) by molecule degradation processes, in accordance with the model of Miller et al. (2010).

3.2. Sensitivity analysis

As a second assessment of the robustness of the model, we performed a sensitivity analysis. We changed all parameters by 25% and evaluated four results, namely the maximal HMOX1 value during simulation (MaxHMOX1), the maximal ROS value during simulation (MaxROS), the time needed for a complete removal of ROS (TimeROSremoved) and the ROS value at 30 min after exposure has begun (ROS at 0.5 h). Fig. 2 shows the results with 25% lower (first sequence of parameters) and 25% higher parameter values (second sequence of parameters). None of the models is overly sensitive; the model outcomes in general do not change more than 10% (all points within the dotted lines, Fig. 2), with a few exceptions which we will discuss in the next Section 3.3.

In all models, the MaxHMOX1 value is the most sensitive result for a change in parameter values, whereas AP-1 is (across the result values) the most sensitive model to parameter changes for MaxHMOX1. The parameters that affect MaxHMOX1 most are: k4 the translation rate; l4 the mRNA degradation rate; k8 the transcription rate; and k10 ROS cleanup rate at binding to HMOX1. MaxHMOX1 increases with lowering the mRNA degradation rate l4 and ROS cleanup rate k10 and it decreases with lowering the translation rate k4 and transcription rate k8, and vice versa for the second sequence of parameters where the values are 25% higher. The change in MaxHMOX1 with k10 is indirect; ROS is removed to a lesser extent, therefore more HMOX1 is induced while at the same time the HMOX1_ROS complex dissociation rate is lower, preventing HMOX1 from degradation. This is because in our model, we assume that complexes are more stable than non-complexed molecules (Szymanska and Zylicz, 2009).

Maximum ROS values (MaxROS) are mostly within 10% of the original value, except for parameter k11 in the HSF1 model, which stands for the DP production from ROS. If this rate is lowered, ROS increases upto a higher level, just exceeding 10% and vice versa.

In all models, the time until complete ROS removal (TimeROSremoved) is sensitive for the parameter k10 (the ROS removal rate at binding to HMOX1). If the removal rate is lowered, it takes more time for the systems to remove ROS, and vice versa.

Early ROS (ROS at 0.5 h) is the least sensitive parameter, because all outcomes are within 10% of the original value, except for the NRF2 model which is sensitive for a change in k6, which is the rate for preferred dimer synthesis by associated dissociation of a non-preferred existing dimer (i.e. AB + C → A + BC). This has a direct link to the initial binding of ROS to BACH1 and KEAP1 in this model while dissociating, respectively, ARE and NRF2, as this lowers the amount of free ROS. If this rate is slower, the ROS at 30 min increases, and vice versa.

Overall, it can be seen in Fig. 2 that the model outcomes are in general not very sensitive to changes in parameter values. Changes

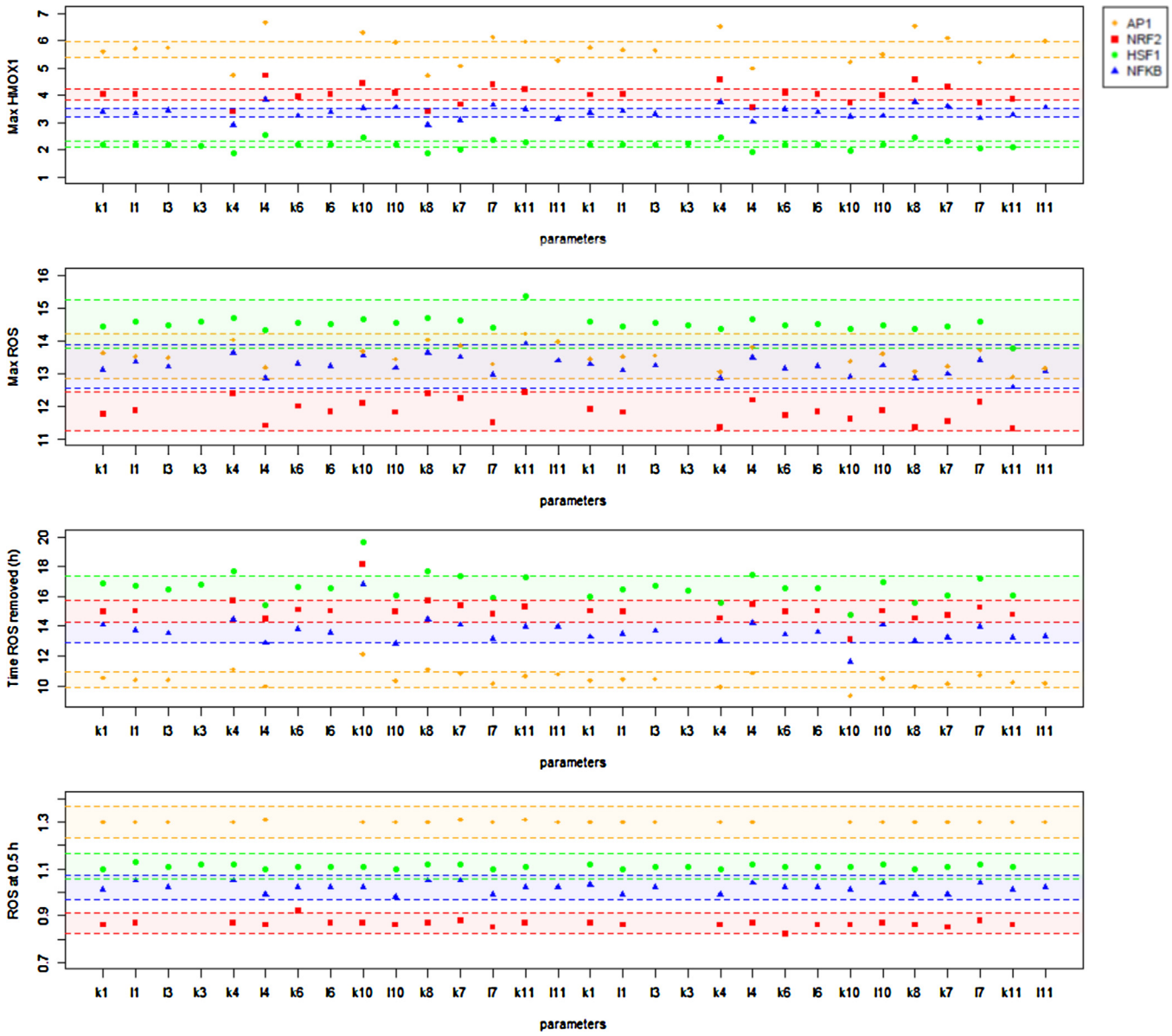

Fig. 2. Sensitivity analysis of all parameters used in the models at a 25% increase (left part of the figure) or a 25% decrease (right part of the figure). The models are evaluated on maximal total HMOX1 value (MaxHMOX1), maximal free ROS value (MaxROS), time until total ROS cleanup (TimeROSremoval) and free ROS at 30 min after the initiation of exposure (ROS at 0.5 h). The dotted lines depict the 10% change interval from the results at default value (see Table 1 for parameters and Table 3 for results at default value).

in parameter values also do not change the relative rank between the models in these outcomes.

3.3. Model results at standard parameter values

From Fig. 2 it can be observed that overall, the fastest molecular circuit to clean up ROS is the AP-1 circuit. The kinetics of all molecules in this circuit are depicted in Fig. 3. Although AP-1 in Fig. 3B is fast to clean up ROS, it is not the most efficient system, as it induces a superfluous amount of HMOX1. Moreover, it is not the best system to reduce the peak level of ROS and also it is the system that is the last to slow down the initial ROS increase at half an hour after exposure. The AP-1 (and the HSF1) system has a di- (or tri- for HSF1) merization step, resulting in an equilibrium where some of the constituents are dimerized and functional, and some are monomeric and non-functional. This reduces the efficiency of the systems, leading to higher initial and maximal ROS values. When in the AP-1 system JUN and FOS proteins increase because of their increased transcription (see Fig. 1 for the route of activation) this slow start is made up for, making it fast in its final cleanup of ROS.

The NF-κB system in Fig. 3D is a more efficient system as it cleans up ROS moderately fast while not inducing HMOX1 up to a very high level. Also, the peak dose of ROS is moderate. IκK is ready to bind to IκBα as soon as it is phosphorylated, which in our model is instantaneous (as a function of the ROS increment); making it a fast process.

HSF1 in Fig. 3A takes the longest to clean up ROS. This is because this transcription factor is triggered by DP, which we introduce at a lower signal than ROS (30% vs. 70% of the total stress input). Moreover, HSF1 needs to trimerize before it can bind to the promoter site of HMOX1, slowing down this process and reducing the number of functional molecules to bind to its promoter site HSE (heat shock sequence element) by threefold. Peak ROS values are also the highest in this system.

NRF2 in Fig. 3C is most apt to keep the peak dose of ROS low. In this system, ROS immediately binds to KEAP1 and BACH1,

Table 2
Molecules in all modelled molecular circuitries and their full names or descriptions.

Molecule	Description
HMOX1	Heme oxygenase 1
mHMOX1	Heme oxygenase 1 mRNA
HSF1 model	
HSP70	Heat shock protein 70
mHSP70	Heat shock protein 70 mRNA
HSF	Heat shock factor
HSE	Heat shock sequence element
NFKB model	
IKBA	Inhibitor of κB: α
mIKBA	Inhibitor of κB: α mRNA
IKK	IκB kinase
NFKB	Nuclear factor κ-light-chain-enhancer of activated B cells
KBM	NF-κB sequence element
NRF2 model	
NRF2	Nuclear factor erythroid 2–related factor 2
BACH1	Basic leucine zipper transcription factor 1
KEAP1	Kelch-like ECH-associated protein 1
ARE	Antioxidant response element
AP-1 model	
JUN	*c*-JUN
mJUN	*c*-JUN mRNA
FOS	*c*-FOS
mFOS	*c*-FOS mRNA
AP1	Activator protein 1
TPE	AP-1 transcription factor binding site element
TFB	Transcription factor binding site element

preventing them from binding until ROS is disengaged by HMOX1, with both the KEAP1 and BACH1 loops inducing HMOX1 transcription. Immediately after ROS induction, the NRF2 system is able to clean up some of the free ROS. It does take a longer time for this system to eliminate all ROS than is the case for for AP-1 and NF-κB. This is because ROS is in conformation with KEAP1 and BACH1, and in our model is not degraded actively in that conformation (see also Szymanska and Zylicz, 2009).

3.4. Different stress scenarios

For a further comparison of the TF molecular circuits, we evaluated these circuits under different stress scenarios. To this end, we changed the stress regime from low to high stress by changing the total stress input, and from short to long exposure to stress by changing the exposure time.

AP-1 reacts most strongly to increased levels of stress, inducing the largest increase in MaxHMOX1. HSF1 is the least responsive (Fig. 4A). For MaxROS the reaction to increased stress is mostly similar between all four models (Fig. 4B). The time until complete ROS removal shows some interesting results for AP-1, as at higher stress AP-1 retains its ability to quickly remove ROS, whereas for the other three models TimeROSremoval increases over time (Fig. 4C). ROS at 0.5 h and MaxROS are not differently affected between the models by an increase in stress (Fig. 4D).

With an increase in exposure duration, MaxHMOX1 is not affected (Fig. 4E). MaxROS however, decreases with the exposure period (Fig. 4F). This is because the same amount of ROS production is spread out over a prolonged period of time. TimeROSremoval increases slightly with exposure time, and increases most for AP-1 (Fig. 4G). Early ROS (ROS at 0.5 h) is lower with an increase in exposure time, with an exponential decrease rather than the more linear decrease observed for MaxROS. The decrease is again a consequence of spreading total ROS over a longer time period. This decrease is similar for all four models (Fig. 4H).

3.5. All models combined

So far, we have evaluated the systems to induce HMOX1 separately. By combining the molecular circuits we now assess which transcription factor is most apt to react to ROS exposure given the simultaneous presence of the other systems. The results, simulated with parameters at default parameters (Table 1) are in Table 3.

All models combined can handle a larger ROS exposure compared to individual models, as the four transcription factors transcribe HMOX1 at their respective transcription initiation sites and we assume the effect is additive. In the combined model the maximum HMOX1 value is higher than in any of the single models. However, the induction is not completely additive. In the separate model, AP-1 alone already has an induction of about 5.7 and combining the models only adds 2.57 to that. Moreover, as expected, in the models combined, MaxROS is lower than in any of the separate models.

Interestingly, TimeROSremoval is about 2 h longer than the time the AP-1 system alone needs for ROS cleanup (see Fig. 2). This is because part of ROS is captured by other regulatory factors, such as KEAP1, that lead to part of the overall response being channelled into slower acting mechanisms, such as the NRF2 system.

3.6. Physiological role in response to toxicants

To further improve our understanding of how the different transcription factor circuits combined respond to oxidative stress, and with a view to ultimately applying this understanding to systems toxicology modelling for toxicants such as skin sensitizing compounds, we applied four different toxicant exposure scenarios to the model with combined circuits. We want to see the different activities of each transcription factor when these are combined. As a measure for the activities of each of the transcription factors we take the binding of a transcription factor to its promoter site as a measure for transcription factor activity and consequent mHMOX1 induction. Results for different stress scenarios are in Fig. 5.

The four scenarios comprise: (A) the default model, which is the same simulation as in the previous Section 3.5 and corresponding to the last column of Table 3, (B) a slower stress induction (mimicking less reactive or less potent compounds), (C) preferentially protein denaturing compounds (DP_{part} set to 0.9, ROS_{part} set to 0.1), (D) tenfold increased stress input (mimicking a high toxicant dose; $EXP_{tot} = 300$). In Fig. 5A we observe that AP-1 returns to steady state slowest and 'overshoots' the stress in the default scenario. This is because this transcription factor undergoes dual activation by both phosphorylation and transcription, and the molecules take some time to degrade. HSF1 returns to steady state values slowly too, because of its trimerization state. In Fig. 5B, simulating a slow increase of stress, we only see a shift in the activation of transcription factors to a later time point and not so much a difference in maximum activity between the transcription factors. At high DP_{part} in Fig. 5C we see that HSF1 is the predominantly active system, with NRF2 having the least activity. In Fig. 5D the stress is so high that we observe an induction of AP-1, NRF2, and HSF1 to a maximum value. This maximum value is for all TF_DNA complexes lower than 1, the theoretical maximum. This is due to an equilibrium reaction connecting to other conformations. Of course, the molecule HSF3_HSE has a theoretical maximum of 0.33, as the molecule (as all molecules in the model) is initialized at unity and trimerizes, thereby reducing the final functional transcription factor by threefold. NF-κB is the only molecular circuit that does not maximize its TF_DNA complex as it only reacts to the signal *S* (see Fig. 5D), which is ROS induction, and not to the total ROS present in the system, in other words the state.

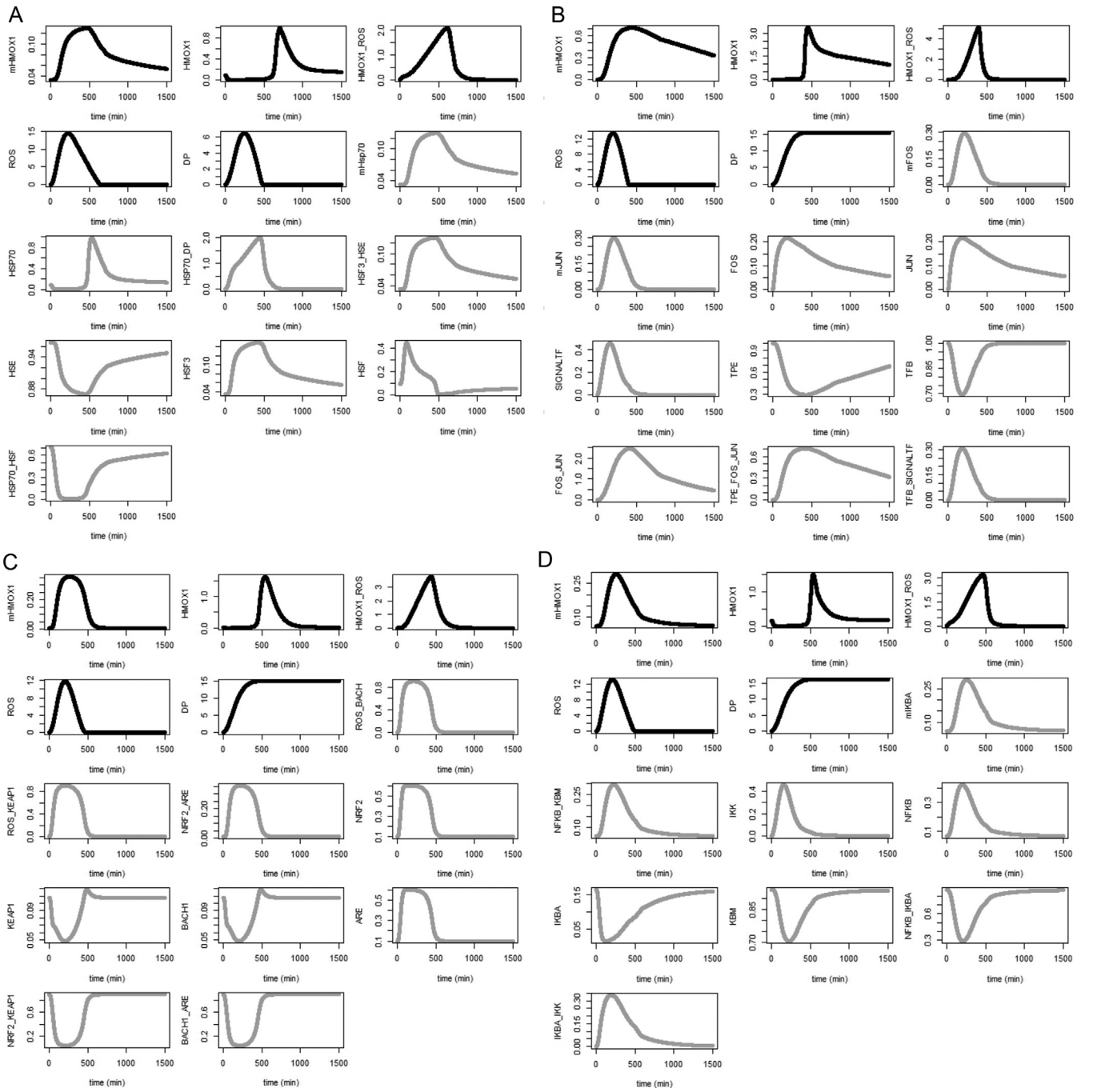

Fig. 3. Kinetics of molecules and complexes over time for the four molecular circuits to induce HMOX1, at standard parameter values (see Table 1). Shown in this figure is the behaviour of molecules resulting from stress exposure according to formula 1, at $t = 0$. The system already has reached steady state at that point (not shown). (A) The HSF1 molecular circuit. (B) The AP-1 molecular circuit. (C) The NRF2 molecular circuit. (D) The NF-κB molecular circuit. For explanation of the names of molecules, see Table 2. The first five boxes in each panel represent common molecule (-complexes) that can be compared between the circuits. In reading order these are: mHmox1, HMOX1, HMOX1_ROS complex, ROS, DP. Please note that these molecules can also be part of other, unique complexes per circuit.

In general, we see an increased activity of HSF1 in all simulations. As DP is a by-product of ROS, it is always produced. Both HSF1 and AP-1 are slow to return to steady state. NRF2 and NF-κB return to steady state more quickly. In all simulations NRF2 returns to steady state the fastest, as the molecular circuit is directly dependent on the ROS present in the system (Table 4).

4. Discussion

Although HMOX1 is an important molecule to prevent irreversible damage to cells caused by reactive oxygen species (ROS), much is unknown about its induction. To evaluate the kinetics of HMOX1 induction by its four transcription factors (Alam and Cook, 2007), we have made mathematical simulation models of the molecular circuits of HSF1, AP-1, NRF2, and NF-κB. All four transcription factors are capable of removing ROS by their capability of inducing HMOX1 (Alam and Cook, 2007). How these circuits compare in terms of speed or efficiency in stress relieve is very hard to deduce from their static graphical representations. Our mathematical models dynamically simulate the states of each molecule in each circuit, enabling the comparison of the kinetics of these circuits. For a proper evaluation of the circuits, they were

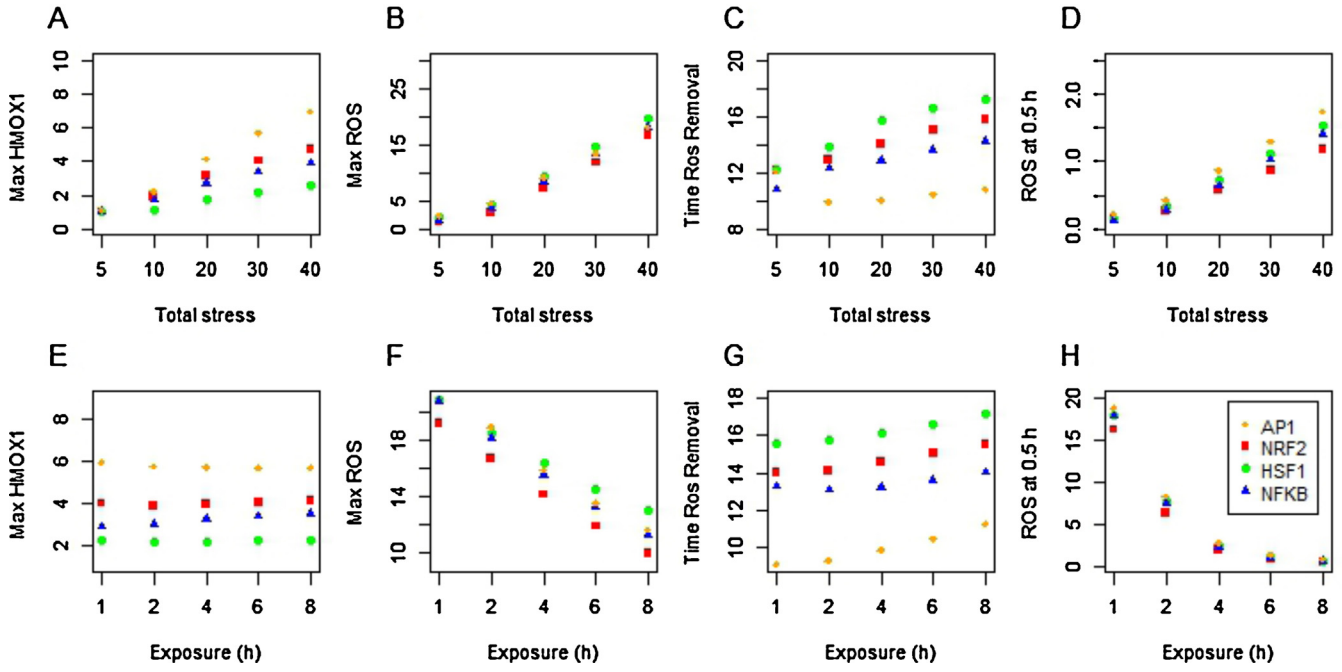

Fig. 4. Effect of stress scenarios involving total stress EXP_{tot} and exposure length EXP_{time} (see Eq. (1)) on the levels of read-out parameters MaxHMOX1, MaxROS, TimeROSRemoval, and ROSat0.5, for the different molecular circuits. See the legend of Fig. 2 for an explanation on these read-out parameters.

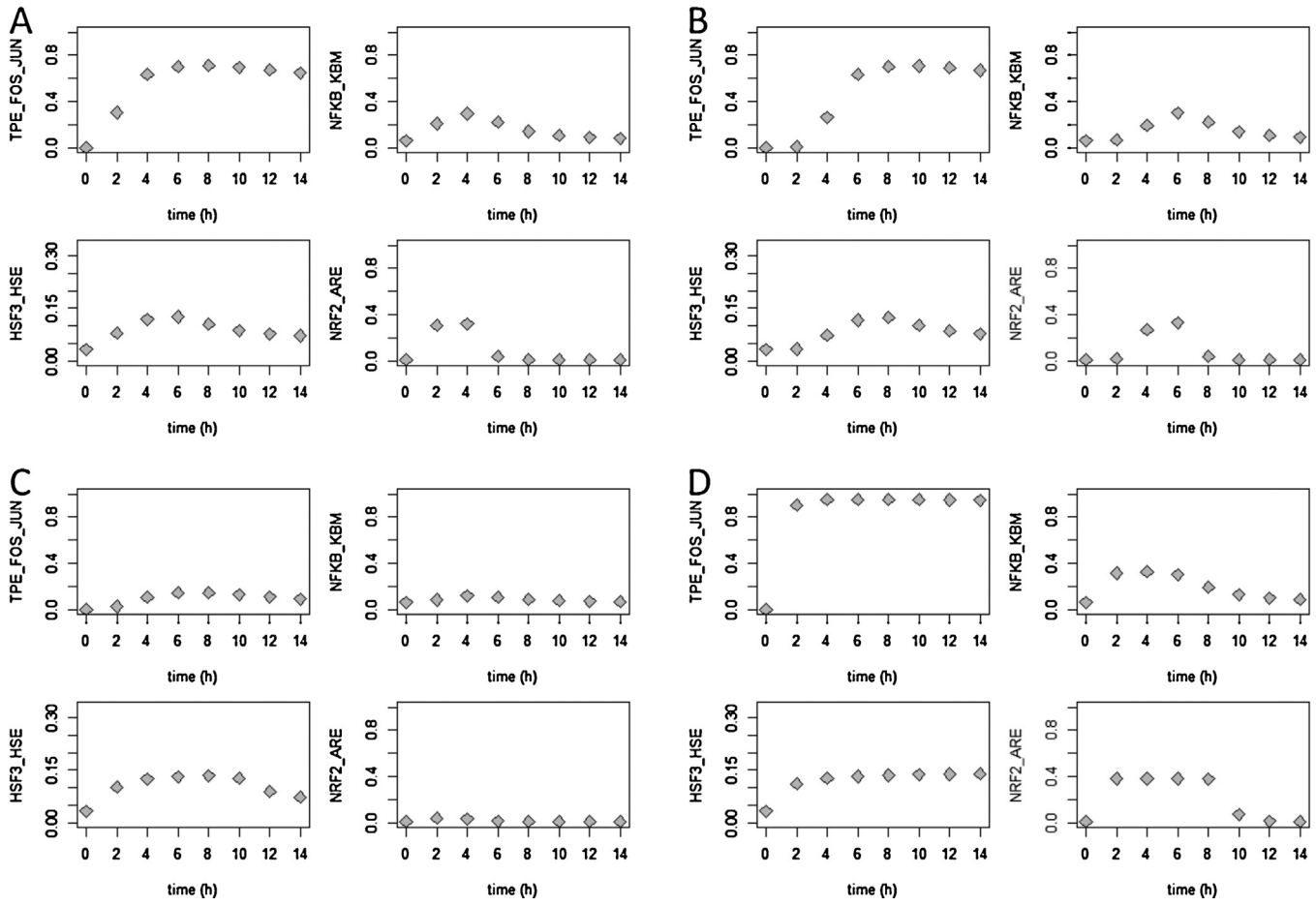

Fig. 5. The activities of TFs (i.e. the fraction of TFs bound to their binding sites) when all molecular circuits are combined, under different scenarios of stress. (A) At default values (see Table 1). (B) At default values with a slow induction peak of stress (with $p1 = 3$ and $p2 = 1$ instead of the other way around, see Eq. (1)). (C) The part of stress caused by denatured proteins DP_{part} is taken as 0.9 instead of 0.3. (D) Total stress input (see Table 1) is increased to 300 instead of 30.

Table 3
Values of the read-out parameters for all circuits, at default values (Table 1) and all circuits combined, at 8 h of simulation.

	HSF1	AP-1	NRF2	NF-κB	Combined
MaxHMOX1	2.20	5.69	4.03	3.38	8.27
MaxROS	14.51	13.52	11.84	13.21	8.36
TimeROSremoval	16.57	10.52	15.01	13.58	12.82
ROS at 0.5 h	1.11	1.3	0.87	1.02	0.69

modelled at the same level of abstraction and with standardized parameter values per type of biochemical reaction. This is novel with respect to already established models which are hard to compare because of different assumptions on rates and different levels of complexity.

In our models, we observe that all molecular circuits have common as well as unique sensitivities for parameter values, depending on the readout parameter. With a change in parameters of 25%, most read-out parameters (maximum HMOX1, maximum

Table 4
Nonlinear differential equations for all models.

General biochemical reactions	
ROSincr	$=p_0((\mathrm{ROS_{part}} \times \mathrm{EXP_{tot}})/\mathrm{EXP_{time}}) \times (\mathrm{time}/\mathrm{EXP_{time}})\hat{}p_1(1-(\mathrm{time}/\mathrm{EXP_{time}}))\hat{}p_2$
DPincr	$=p_0((\mathrm{DP_{part}} \times \mathrm{EXP_{tot}})/\mathrm{Exp_{time}}) \times (\mathrm{time}/\mathrm{EXP_{time}})\hat{}p_1(1-(\mathrm{time}/\mathrm{EXP_{time}}))\hat{}p_2$
Signincr	=l11(ROSincr)
dHMOX1/dt	=k4 × mHmox1 − k1 × HMOX1 × ROS + k10 × HMOX1_ROS − l10 × HMOX1
dROS/dt	=ROSinc − k10 × HMOX1_ROS − k11 × ROS − k1 × HMOX1 × ROS + l7 × ROS_KEAP1 − k7 × KEAP1 × ROS − k7 × BACH1 × ROS + l7 × ROS_BACH1 − k6 × ROS × NRF2_KEAP1 + l6 × ROS_KEAP1 × NRF2 − k6 × ROS × BACH1_ARE + l6 × ROS_BACH1 × ARE
dHMOX1_ROS/dt	=k1 × HMOX1 × ROS − k10 × HMOX1_ROS
mHmox1/dt	=−l4 × mHmox1 + k8 × TPE_FOS_JUN + k8 × HSF3_HSE + k8 × NRF2_ARE + k8 × NFKB_KBM
dDP/dt	=DPincr + k11 × ROS + l1 × Hsp70_DP − k1 × Hsp70 × DP − k6 × Hsp70_HSF × DP + l6 × Hsp70_DP × HSF − k10 × Hsp70_DP
Submodel 1: HSF1 biochemical reaction network	
dHsp70/dt	=−m1_k1 × Hsp70 × HSF + m1_l1 × Hsp70_HSF − m1_k1 × Hsp70 × DP + m1_l1 × Hsp70_DP − m1_l3 × Hsp70 × HSF3 + m1_k4 × mHsp70 + m1_k10 × Hsp70_DP − m1_l10 × Hsp70
dHSF/dt	=−m1_k1 × Hsp70 × HSF + m1_l1 × Hsp70_HSF − 3 × m1_k3 × HSF × HSF × HSF + 2 × m1_l3 × Hsp70 × HSF3 + m1_k6 × Hsp70_HSF × DP − m1_l6 × Hsp70_DP × HSF
dHsp70_HSF/dt	=m1_k1 × Hsp70 × HSF − m1_l1 × Hsp70_HSF − m1_k6 × Hsp70_HSF × DP + m1_l6 × Hsp70_DP × HSF + m1_l3 × Hsp70 × HSF3
dHsp70_DP/dt	=m1_k1 × Hsp70 × DP − m1_l1 × Hsp70_DP + m1_k6 × Hsp70_HSF × DP − m1_l6 × Hsp70_DP × HSF − m1_k10 × Hsp70_DP
dHSF3/dt	=m1_k3 × HSF × HSF × HSF − m1_l3 × Hsp70 × HSF3 − m1_k7 × HSF3 × HSE + m1_l7 × HSF3_HSE
dHSE/dt	=−m1_k7 × HSF3 × HSE + m1_l7 × HSF3_HSE
dHSF3_HSE/dt	=m1_k7 × HSF3 × HSE − m1_l7 × HSF3_HSE
dmHsp70/dt	=m1_k8 × HSF3_HSE − m1_l4 × mHsp70
Submodel 2: NF-kB biochemical reaction network	
dIKBA/dt	=−m2_k1 × IKBA × NFKB + m2_l1 × NFKB_IKBA − m2_k1 × IKBA × IKK + m2_l1 × IKBA_IKK + m2_k4 × mIKBA − m2_k10 × IKBA_IKK − m2_l10 × IKBA
dIKK/dt	=Signincr + m2_l1 × IKBA_IKK − m2_k1 × IKBA × IKK − m2_k6 × NFKB_IKBA × IKK + m2_l6 × IKBA_IKK × NFKB + m2_k10 × IKBA_IKK − m2_l10 × IKK - m2_l3 × IKK
dNFKB_IKBA/dt	=m2_k1 × NFKB × IKBA − m2_l1 × NFKB_IKBA − m2_k6 × NFKB_IKBA × IKK + m2_l6 × IKBA_IKK × NFKB
dIKBA_IKK/dt	=m2_k1 × IKBA × IKK − m2_l1 × IKBA_IKK + m2_k6 × NFKB_IKBA × IKK − m2_l6 × IKBA_IKK × NFKB − m2_k10 × IKBA_IKK
dNFKB/dt	=−m2_k1 × NFKB × IKBA + m2_l1 × NFKB_IKBA + m2_k6 × NFKB_IKBA × IKK − m2_l6 × IKBA_IKK × NFKB − m2_k7 × NFKB × KBM + m2_l7 × NFKB_KBM
dKBM/dt	=−m2_k7 × NFKB × KBM + m2_l7 × NFKB_KBM
dNFKB_KBM/dt	=m2_k7 × NFKB × KBM − m2_l7 × NFKB_KBM
dmIKBA/dt	=m2_k8 × NFKB_KBM − m2_l4 × mIKBA
Submodel 3: NRF2 biochemical reaction network	
dNRF2/dt	=−m3_k1 × NRF2 × KEAP1 + m3_l1 × NRF2_KEAP1 + m3_k6 × NRF2_KEAP1 × ROS − m3_l6 × ROS_KEAP1 × NRF2 − m3_k7 × NRF2 × ARE + m3_l7 × NRF2_ARE
dBACH1/dt	=−m3_k1 × ARE × BACH1 + m3_l1 × BACH1_ARE + m3_l7 × ROS_BACH1 − m3_k7 × BACH1 × ROS
dARE/dt	=−m3_k1 × BACH1 × ARE + m3_l1 × BACH1_ARE − m3_k7 × NRF2 × ARE + m3_l7 × NRF2_ARE + m3_k6 × BACH1_ARE × ROS − m3_l6 × ROS_BACH1 × ARE
dKEAP1/dt	=−m3_k1 × NRF2 × KEAP1 + m3_l1 × NRF2_KEAP1 + m3_l7 × ROS_KEAP1 − m3_k7 × KEAP1 × ROS
dNRF2_KEAP1/dt	=m3_k1 × KEAP1 × NRF2 − m3_l1 × NRF2_KEAP1 − m3_k6 × NRF2_KEAP1 × ROS + m3_l6 × ROS_KEAP1 × NRF2
dBACH1_ARE/dt	=m3_k1 × BACH1 × ARE − m3_l1 × BACH1_ARE − m3_k6 × BACH1_ARE × ROS + m3_l6 × ROS_BACH1 × ARE
dNRF2_ARE/dt	=m3_k7 × NRF2 × ARE − m3_l7 × NRF2_ARE
dROS_KEAP1/dt	=m3_k7 × KEAP1 × ROS − m3_l7 × ROS_KEAP1 + m3_k6 × NRF2_KEAP1 × ROS − m3_l6 × ROS_KEAP1 × NRF2
dROS_BACH1/dt	=m3_k7 × BACH1 × ROS − m3_l7 × ROS_BACH1 + m3_k6 × BACH1_ARE × ROS − m3_l6 × ROS_BACH1 × ARE
Submodel 4: AP-1 biochemical reaction network	
phosphorylation of present FOS up to '1'	if(FOS < 1){FOSphincr < −Signincr}else {FOSphincr < −0}
phosphorylation of present JUN up to '1'	if(JUN < 1) {JUNphincr < −Signincr} else {JUNphincr < −0}
dFOS/dt	=FOSphincr − m4_k1 × JUN × FOS + m4_l1 × FOS_JUN + m4_k4 × mFOS − m4_l10 × FOS − m4_l3 × FOS
dJUN/dt	=JUNphincr − m4_k1 × JUN × FOS + m4_l1 × FOS_JUN + m4_k4 × mJUN − m4_l10 × JUN − m4_l3 × JUN
dSIGNALTF/dt	=Signincr + m4_k7 × TFB_SIGNALTF − m4_l7 × TFB × SIGNALTF − m4_l10 × SIGNALTF − m4_l3 × SIGNALTF
dTPE/dt	=−m4_k7 × FOS_JUN × TPE + m4_l7 × TPE_FOS_JUN
dTFB/dt	=−m4_k7 × SIGNALTF × TFB + m4_l7 × TFB_SIGNALTF
dTPE_FOS_JUN/dt	=m4_k7 × FOS_JUN × TPE − m4_l7 × TPE_FOS_JUN
dTFB_SIGNALTF/dt	=m4_k7 × SIGNALTF × TFB − m4_l7 × TFB_SIGNALTF
dFOS_JUN/dt	=m4_k1 × FOS × JUN − m4_l1 × FOS_JUN − m4_k7 × FOS_JUN × TPE + m4_l7 × TPE_FOS_JUN
dmJUN/dt	=m4_k8 × TFB_SIGNALTF − m4_l4 × mJUN
mFOS/dt	=m4_k8 × TFB_SIGNALTF − m4_l4 × mFOS

ROS, time to remove ROS altogether, initial removal of ROS) changed within 10% of their original value. The most sensitive model was AP-1, especially with respect to the readout parameter maximum HMOX1.

In our models, two circuits (HSF1 and AP-1) seem especially suited for long-term removal of stress. These systems are slow to return to their steady-state, making them robust to possible renewed exposures to stress. Between the two, HSF1 is specialised to alleviate the stress induced by denatured proteins, and AP-1 is suitable to remove oxidative stress by responding to a danger signal related to this stress. Especially AP-1 functions here as a general-purpose stress response protein, with an effective stress response at the expense of efficiency. The two other molecular circuits that can alleviate stress (NF-κB and NRF2) respond in a more transient way and deactivate soon after the stress factor ROS has been removed. This makes them efficient molecular circuits that do not waste energy on superfluous HMOX1 production. NRF2 seems most appropriate for cellular homeostasis by adaptive and efficient regulation of ROS levels. In terms of pathology, the model directs to AP-1 as a likely candidate for producing superfluous HMOX1, as well as a being the circuitry that can clean up ROS the fastest. AP-1 was not sensitive to the amount of stress, as the time to clean up ROS remained almost the same for all of the simulated stress levels. NRF2 is the circuitry that keeps maximum free ROS lowest at any time. Making explicit such behaviour, this paper provides a first step towards kinetic understanding of the regulation of HMOX1 from the perspective of the different transcription factor circuitries.

When combining the molecular circuits of the four transcription factors into a single system of differential equations, we simulated several scenarios. Not surprisingly, the maximum amount of ROS was reduced with all TFs combined, and the maximum HMOX1 induction increased compared to any single model. Less anticipated was the fact that with all models combined the time to remove ROS did not decrease compared to the fastest single model AP-1. This could be accounted to the NRF2 system, in which part of ROS is complexed with KEAP1 and BACH1 and not actively degraded. In a new simulation, the shape of the stress increment proved to influence the responsiveness of all models only to a small extent, except in that a slow increment delayed the transcription factor binding to DNA. In contrast to these results, Szymanska and Zylicz (2009) showed that in the HSF1 system there was virtually no response to a slow increment of temperature with associated DP formation. However, during the course of slow increase in temperature less DP was formed than during fast elevation of temperature. This may be a cause of their contrasting results compared to our results, where total DP was fixed and only the peak was delayed.

There are points to be raised regarding modelling and comparing four different molecular circuits to induce HMOX1. One general decision to make when modelling is the level of complexity within a model. While sufficient detail should be built into a model, it should not become too complex. With too little simplifications, the tractability and interpretation of model results will be difficult. This is because with too many (interacting) parameters, the model can become overly sensitive to changes in input parameters. Moreover, a vast amount of data will have to be gathered for parameterization. A solution is to only model explicitly those molecules that are directly affected by the stimulus. Other molecules are assumed to be in steady state. This approach was taken by Szymanska and Zylicz (2009) in their model on heat shock response, which we have taken as a template.

Another general impediment for model construction is finding values for all the parameters. Kinetic data is often not available. Where kinetic data is available, it is often from a specific system, which may not accurately reflect the kinetics in the system of interest. However, even if exact values are not easy to obtain, it is often satisfactory to know the relative time scales of the reactions. For example, kinase/phosphatase reactions are very fast reactions occurring over timescales that range from fraction of a second to seconds, whereas protein synthesis takes several minutes. Degradation rates are dependent on protein type but fortunately, there is usually information available on protein half-lives that can be used to calculate the degradation rate. Unknown rates can be fitted to resemble the known situation, such as a preferred state as dimer/monomer. We have taken this approach for all transcription factor models, based on the template by Szymanska and Zylicz (2009).

Additionally, the completeness or simplicity of the models can be a limiting factor. We have modelled the four molecular circuits of HSF1, AP-1, NRF2, and NF-κB according to the basic systems agreed upon in literature. However, in some instances in literature, extensions to these circuits have been suggested or proven in particular model systems. For the systems in which these extensions have been proven to significantly influence HMOX1 kinetics, it would be worthwhile to extend the model circuits with these additional elements. For instance, in AP-1, Lamin could play a role in harbouring excess FOS, removing it from the system and limiting the formation of the AP-1 complex (Ivorra et al., 2006), so transcription of HMOX1 is stalled. For NF-κB an extra inactivation of IκK by the protein A20 (Lipniacki et al., 2004) has been proposed, which would result in returning the system to its steady state after stress faster than in the current model circuit. Additional NF-κB response downregulation mechanisms, by modulating the signalling cascades, have been discussed by Ruland (2011). Lastly, some of the the stress-activated recognition sites contained within the *Hmox1* promoter overlap somewhat in sequence, making binding non-exclusive (Alam and Cook, 2007).

In conclusion, we have modelled the abilities of four molecular circuits in their efficiency to remove the inducers of stress, ROS and DP, with the aim of comparing their kinetics. Our approach of modelling at similar levels of abstraction and rates enables to make inferences on the systems and compare them with only the topology differing. This resulted in the identification of HSF1 and AP1 as two systems capable of long-term ROS removal and NRF2 and NF-κB as more transient systems. It is well possible that the systems have evolved in some way to overcome the limitations in their circuitry in the shape of extra regulation or adaptations in concentration of molecules. These simulations should therefore not be considered as definitive outcomes, but rather to spur hypotheses on which system is inherently suitable to alleviate different kinds of physiological stress scenarios based on their topology.

Acknowledgements

This work was supported by a grant of the Netherlands Genomics Initiative/Netherlands Organization for Scientific Research (050-060-510) to the Netherlands Toxicogenomics Centre. We thank Wils A. L. Pronk and Sebastiaan Wesseling for their help concerning biochemical reaction rates.

References

Alam, J., Cook, J.L., 2007. How many transcription factors does it take to turn on the heme oxygenase-1 gene? Am. J. Respir. Cell. Mol. Biol. 36, 166–174.

Caton, B.P., Foin, T.C., Hill, J.E., 1999. A plant growth model for integrated weed management in direct- seeded rice: III. Interspecific competition for light. Field Crop. Res. 63, 47–61.

Hoffmann, A., Levchenko, A., Scott, M.L., Baltimore, D., 2002. The IkB–NFkB signalling module: temporal control and selective gene activation. Science 298, 1241–1245.

Ihekwaba, A.E.C., Broomhead, D.S., Grimley, R.L., Benson, N., Kell, D.B., 2004. Sensitivity analysis of parameters controlling oscillatory signalling in the NFkB pathway of IKK and IkBa. Syst. Biol. 1 (1), 93–103.
Ivorra, C., Kubicek, M., González, J.M., Sanz-González, S.M., Alvarez-Barrientos, A., O'Connor, J.E., Burke, B., Andrés, V., 2006. A mechanism of AP-1 suppression through interaction of c-Fos with lamin A/C. Genes Dev. 20 (3), 307–320.
Karin, M., 1995. The regulation of AP-1 activity by mitogen-activated protein kinases. J. Biol. Chem. 270 (28), 16483–16486.
Lipniacki, T., Paszek, P., Brasier, A.R., Luxon, B., Kimmel, M., 2004. Mathematical model of NF-kB regulatory module. J. Theor. Biol. 228, 195–215.
Miller, G.M., Ogunnaike, B.A., Schwaber, J.S., Vadigepalli, R., 2010. Robust dynamic balance of AP-1 transcription factors in a neuronal gene regulatory network. BMC Syst. Biol. 4, 171.
Natsch, A., 2009. The Nrf2-Keap1-ARE toxicity pathway as a cellular sensor for skin sensitizers- functional relevance and a hypothesis on innate reactions to skin sensitizers. Toxicol. Sci. 113, 284–292.
Peper, A., Grimbergen, C.A., Spaan, J.A.E., Souren, J.E.M., van Wijk, R., 1998. A mathematical model of the hsp70 regulation in the cell. Int. J. Hyperthermia 14 (1), 97–124.
Petre, I., Mizera, A., Hyder, C.L., Mikhailov, A., Eriksson, J.E., Sistonen, L., Back, R.-J., 2009. A new mathematical model for the heat shock response. In: Condon, A. (Ed.), Algorithmic Bioprocesses, Natural Computing Series. Springer, Heidelberg, Berlin.
Pronk, T.E., van Someren, E.P., Stierum, R.H., Ezendam, J., Pennings, J.L.A., 2013. Unraveling toxicological mechanisms and predicting toxicity classes with gene dysregulation networks. J. Appl. Toxicol. 33 (12), 1407–1415.
Reichard, J.F., Motz, G.T., Puga, A., 2007. Heme oxygenase-1 induction by NRF2 requires inactivation of the transcriptional repressor BACH1. Nucleic Acids Res. 35 (21), 7074–7086.
Rice, N.R., Ernst, M.K., 1993. In vivo control of NF-kB activation by IkBa. EMBO J. 12 (12), 4685–4695.
Rieger, T.R., Morimoto, R.I., Hatzimanikatis, V., 2005. Mathematical modeling of the eukaryotic heat-shock response: dynamics of the hsp70 promoter. Biophys. J. 88, 1646–1658.
Ruland, J., 2011. Return to homeostasis: downregulation of NFkB responses. Nat. Immunol. 12 (8), 709–714.
Ryter, S.W., Alam, J., Choi, A.M.K., 2006. Heme oxygenase-1/carbon monoxide: from basic science to therapeutic applications. Physiol. Rev. 86, 583–650.
Saito, K., Miyazawa, M., Nukada, Y., Sakaguchi, H., Nishiyama, N., 2013. Development of an in vitro skin sensitization test based on ROS production in THP-1 cells. Toxicol. In Vitro 27 (2), 857–863.
Suttner, D.M., Dennery, P.A., 1999. Reversal of HO-1 related cytoprotection with increased expression is due to reactive iron. FASEB J. 13 (13), 1800–1809.
Szymanska, Z., Zylicz, M., 2009. Mathematical modelling of heat shock protein synthesis in response to temperature change. J. Theor. Biol. 259, 562–569.
Vandebriel, R.J., Pennings, J.L., Baken, K.A., Pronk, T.E., Boorsma, A., Gottschalk, R., Van Loveren, H., 2010. Keratinocyte gene expression profiles discriminate sensitizing and irritating compounds. Toxicol. Sci. 117 (1), 81–89.
Van der Veen, J.W., Pronk, T.E., van Loveren, H., Ezendam, J., 2013. Applicability of a keratinocyte gene signature to predict skin sensitizing potential. Toxicol. In Vitro 27 (1), 314–322.
Walther, M., De Caul, A., Aka, P., Njie, M., Amambua-Ngwa, A., Walther, B., Predazzi, I. M., Cunnington, A., Deininger, S., Takem, E.N., Ebonyi, A., Weis, S., Walton, R., Rowland-Jones, S., Sirugo, G., Williams, S.M., Conway, D.J., 2012. HMOX1 gene promoter alleles and high HO-1 levels are associated with severe malaria in Gambian children. PLoS Pathog. 8 (3), e1002579.